One-Dimensional Transport Calculation of Energy- and Space-Distribution of Neutral Particles in a High Temperature Plasma

By

Hoi-tung YIP*, Hiroshi HISHIHARA*, Shukuro YANO**

(Received September 30, 1978)

Abstract

The transport equation for neutral particles in a high temperature plasma was numerically solved in a one-dimensional phase space. Close correlation has been found between the spectra of the emerging neutral flux and the plasma parameters. The numerical results show that the asymptotic temperature, which is determined from the calculated spectrum of the emerging neutral flux, varies from about 70 % to 95 % of the maximum ion temperature for the realizable plasma conditions. The reflection coefficient of the wall and the profile of the ion temperature of the plasma do not bring any important influence to the spectrum of emerging neutral flux.

1. Introduction

The energy spectrum of fast neutral particles emerging from a high temperature plasma is closely correlated with the ion temperature T_i, the electron temperature T_e, the plasma density n, and their spatial distributions in the plasma column. Therefore, it is considered that the energy analysis of of those neutral particles escaping from the plasma is an effectual method of the plasma diagnostics,[1,2] provided that the above mentioned correlations of the spectrum with the plasma parameters are established.

The purpose of the present study is to find these correlations in the simplest case of one-dimensional plasma geometry, and hence to give a more accurate estimation for the ion temperature measurement in the next generation tokamaks.

Dnestrovskii, Kostomarov, and Pavlova[3] treated the neutral transport by a one-dimensional slab geometry. They assumed that, with a charge-exchange, a neutral atom is generated with an energy equal to the ion temperature and with an equal probability of travelling in the $\pm x$-direction. Thus, the neutral distribution

* Department of Nuclear Engineering.
** Kobe University of Mercantile Marine.

$f(x, v)$ in the layer $-a<x<a$ satisfies the following equation:

$$v\frac{\partial f}{\partial x}+sf = FN_n \cdot \frac{1}{2v_0}\left[\delta\left(\frac{v-v_i}{v_0}\right)+\delta\left(\frac{v+v_i}{v_0}\right)\right] \qquad (1)$$

where

$$s = s(x) = F+10^{-3}\sigma_e n v_e\,, \quad F = F(x) = 0.04\sigma_p n v_i\,,$$
$$v_i = v_i(x) = 1.4\times 10^6\sqrt{T_i(x)/p}\,, \qquad v_e = 0.6\times 10^8\sqrt{T_e(x)}\,,$$
$$N_n = N_n(x) = \int_{-\infty}^{\infty} f(x, v)dv\,.$$

They introduced a boundary condition in the form of a delta-function as

$$f(\pm a, v) = \frac{A_0}{v_0}\delta\left(\frac{v\pm v_i}{v_0}\right) \qquad (1)$$

where v_0 and A_0 are the thermal velocity and the density of the neutrals in the vacuum, respectively.

Thus, they have derived an integral equation for the neutral density N_n

$$N_n(x) = N_0(x)+\int_0^a K(x, \xi)N_n(\xi)d\xi\,, \qquad (0<x<a)\,, \qquad (3)$$

where $N_0(x)$ corresponds to the density of the neutrals in the plasma without considering the secondary neutrals which appeared as a result of the charge-exchange. Hence, the kernel is written as follows:

$$K(x, \xi) = \frac{1}{2}\frac{F(\xi)}{v_i(\xi)}\{\phi(\xi, x, v_i(\xi)\mathrm{sign}(x-\xi)) + \phi(0, \xi, v_i(\xi))\phi(0, x, v_i(\xi))\}\,, \qquad (4)$$

where $\phi(\xi, x, v) = \exp\left[\frac{-1}{v}\int_\xi^x sdx'\right]$.

Rehker and Wobig[4] also derived an integral equation for N_n. They treated the boundary condition in several reflection mechanisms of the neutral particles from the wall. Then they compared the results obtained with a Maxwellian distribution of ions with those of a delta-like distribution.

Table 1 shows some characteristics of the mathematical models used for the

Table 1. Solutions for neutral transport

Authors	Geometry	Ion velocity distribution	Boundary condition	Numerical method
Dnestrovskii, et al. (1971)	Slab	Delta-function & Maxwellian	Deltafunction	Integral eq., functional iteration for N_n
Rehker et al. (1973)	Slab	Delta-function & Maxwellian	Ideal & dififfuse reflection	Integral eq.

solutions of neutral transport in references 3) and 4).

In this paper, we shall solve the transport equation for the neutral particles in an infinite slab model which is also adopted in references 3) and 4). However, we are going to treat this problem with the following improvements:

(1) Instead of the delta function and the diffuse reflection of the neutrals being treated as a boundary condition in references 3) and 4), we treat the immerging slow neutrals as an equivalently distributed external source.

(2) The infinite difference equation for the transport equation is derived and solved iteratively.

(3) In preparation for the next geneartion tokamak, the influence of the plasma parameters on the emerging neutral spectra is studied systemtically by changing the plasma parameters in wide ranges.

2. Particle interactions in a high temperature hydrogen plasma

Among many kinds of particle interactions which may take place in a high temperature plasma, we shall take into accuont the following three reactions which are considered to be the most important. The first is the ionization of hydrogen atoms by electrons

$$\mathbf{H}+e \rightarrow \mathbf{H}^{+}+2e\,. \tag{5}$$

The second is the charge-exchange between ions and neutral particles

$$\mathbf{H}+\mathbf{H}^{+} \rightarrow \mathbf{H}^{+}+\mathbf{H}\,. \tag{6}$$

The third is the ionization of neutral atoms by ions above 10 keV

$$\mathbf{H}+\mathbf{H}^{+} \rightarrow 2\mathbf{H}^{+}+e\,. \tag{7}$$

Riviere has summarized all the cross-section data for the above interactions, and has presented formulas which fit the experimental data well.[5] We quote the following cross-section formulas from reference 5).

For the ionization of hydrogen atoms by electrons, the cross-section above the threshold energy is given by

$$\sigma_1(E) = 3.519\times 10^{-16} h(E)\,, \tag{8}$$

where $$h(E) = \frac{1}{z}\left(\frac{z-1}{z+1}\right)^{3/2}\left(1+\frac{2}{3}\left(1-\frac{1}{2z}\right)\ln\left(2.7+\sqrt{z-1}\right)\right),$$

with $$z = E/E_0\,,\quad E_0 = 13.605\ \text{eV}\,.$$

For the charge-exchange, the cross-section is given by

$$\sigma_2(E) = \frac{0.6937\times10^{-14}(1-0.155\log_{10}E)^2}{1+0.1112\times10^{-14}E^{3.3}}. \quad (9)$$

For the ionization by ions above 10 keV and below 150 keV, we use the formula

$$\sigma_3(E) = 10^{y(E)}, \quad (10)$$

where $y(E) = -0.8712(\log_{10}E)^2+8.156\log_{10}E-34.833$,

Above 150 keV, we use

$$\sigma_3(E) = 3.6\times10^{-12}E^{-1}\log_{10}(0.1666E) \quad (11)$$

In formulas (8) through (11), the cross-section σ and the relative energy E are expressed in cm^2 and eV, respectively, The cross-sections calculated with these formulas are shown in Figs. 1–3, as a function of the relative energy E.

We take the average of the product σv with respect to the one-dimension al Maxwellian velocity distribution of electrons or ions, and call this the rate coefficient after Riviere,[5]

$$\langle\sigma v\rangle_j = \left(\frac{m_j}{2\pi kT_j}\right)^{1/2}\int_{-\infty}^{\infty}\sigma(|v-v_0|)\,|v-v_0|\exp\left[\frac{-m_jv^2}{2kT_j}\right]dv. \quad (12)$$

In Eq. (12), j indicates the species of the plasma particles concerned, i.e. $j=1$ indicates the electron while $j=2$ indicates the ion. Figures 4 and 5 show the rate coefficient of ionization by electrons and that of the charge-exchange as a function of temperatures of the plasma particles, respecitvely, with the energy of the neutral particles as a parameter.

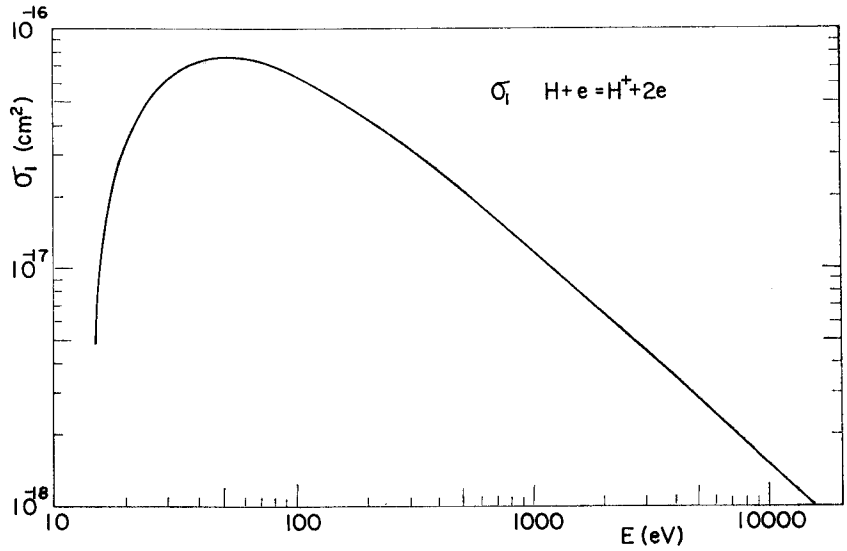

Fig. 1. Cross-section of ionization of atomic hydrogen by electrons.

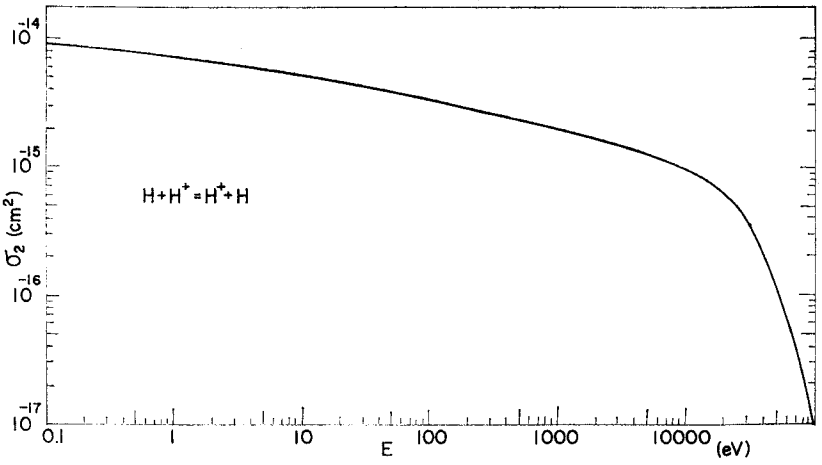

Fig. 2. Cross-section of charge-exhcange between atomic hydrogen and protons.

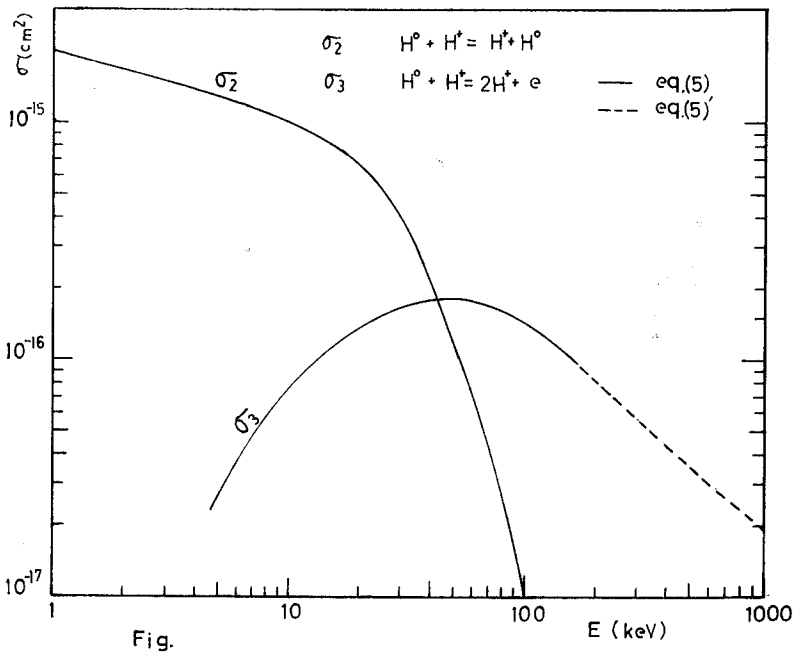

Fig. 3. Cross-sections of charge-exchange and ionization of atomic hydrogen with and by protons, respectively.

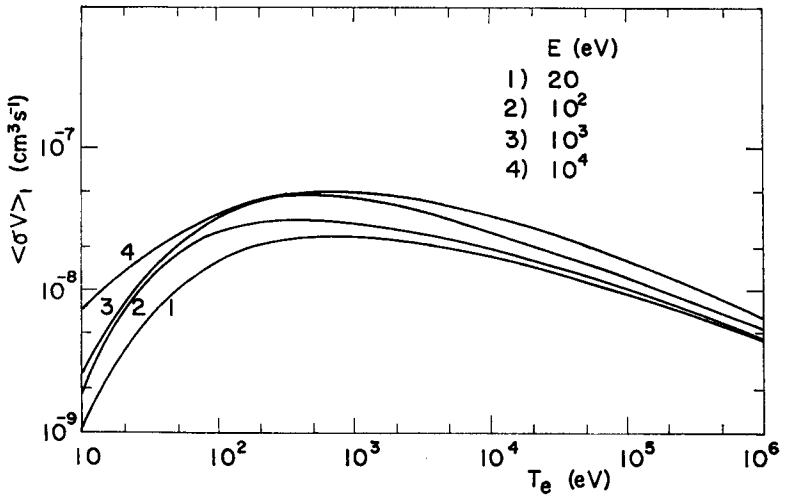

Fig. 4. Rate coefficient of ionization of atomic hydrogen by electrons as a function of the electron temperature.

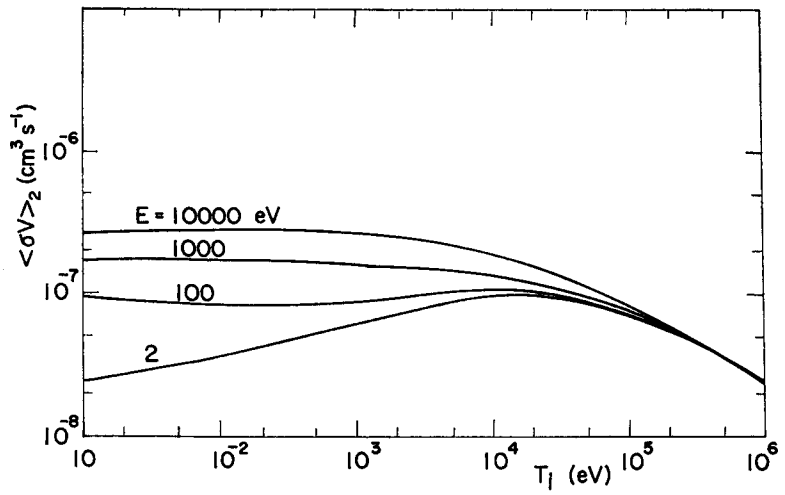

Fig. 5. Rate coefficient of charge-exchange between atomic hydrogen and protons as a function of the ion temperature.

3. Transport equation for neutral particles

The plasma is assumed to be a symmetrical slab with a thickness of $2a$ (Fig. 6). The distribution functions of the neutral particles are written as $f^{\pm}(x, v)$, with the sign $\pm$ indicating the particles moving in the $\pm x$-direction. According to the symmetry of the model, $f^{+}(x, v) = f^{-}(-x, v)$.

The distribution function of the j-species of the plasma particles is assumed to

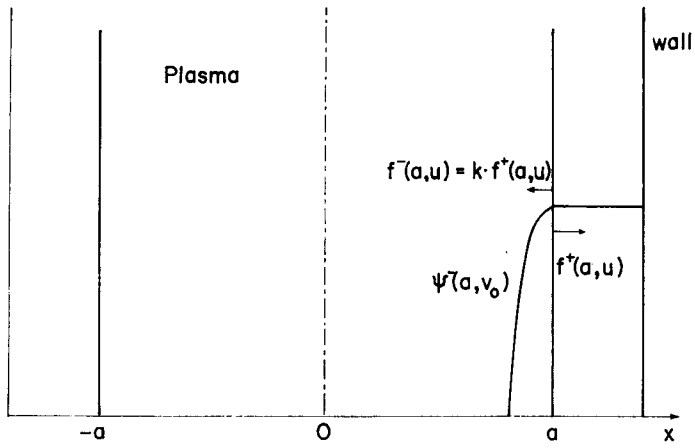

Fig. 6. Geometry assumed.

be $n(x)g_j(x, v)$,

where $$g_j(x, v) = \left(\frac{m_j}{2\pi k T_j(x)}\right)^{1/2} \exp\left[\frac{-m_j v^2}{2k T_j(x)}\right], \qquad (0<v<\infty)$$

is the one-dimensional Maxwellian distribution with the space-dependent temperature $T_j(x)$.

Since $g_j(x, v)$ is defined in half-infinite velocity space $0<v<\infty$, the distribution of ions moving in the $\pm x$-direction is equal to $\frac{1}{2}n(x)g_i(x, v)$.

We also assume that the slow neutrals outside the plasma slab are the external source of neutrals which immerge into the plasma slab from two surfaces of the plasma. The slow neutrals have an energy of 2.2 eV with an equivalent thermal velocity v_0. Thus, the distribution of the slow neutrals in the plasma slab is given by

$$\psi^+(x, v_0) = \psi p(-a \rightarrow x, v_0)$$
$$\psi^-(x, v_0) = \psi p(a \rightarrow x, v_0)$$

where $p(-a \rightarrow x, v_0)$ and $p(a \rightarrow x, v_0)$ are the probabilities for a neutral particle immerging into the plasma from a or $-a$ to reach x without undergoing any collisions, respectively. Because of the symmetry, ψ^+ and ψ^- are related by $\psi^+(x, v_0) = \psi^-(-x, v_0)$. The probability p can be expressed as

$$p(a \rightarrow x, v_0) = \exp\left[-\int_x^a \frac{1}{\lambda} dx'\right],$$

where $1/\lambda = n(x)\langle\sigma v\rangle/v_0$, λ is the mean free path for the sinking process of the slow neutrals in the plasma, and $\langle\sigma v\rangle$ is the total rate coefficient for the same

process.

The sinkage of the neutrals in the plasma is considered to be due to the ionization by electrons and the charge-exchange with the ions. Ionization by ions is neglected here. Because the charge-exchange between the neutrals and the ions is a so-called symmetrical resonant reaction, there is no energy transfer in the reaction.[6] Therefore, the neutrals generated in this reaction will acquire the ion energies. With the above assumptions, we can write down the steady-state transport equation for the neutrals in the plasma as follows:

$$\begin{aligned}\frac{\partial f^{\pm}(x, v)}{\partial x} = & \mp\frac{1}{v} n(x)\langle\sigma v\rangle f^{\pm}(x, v) \\ & \pm\frac{1}{2}\frac{n(x)}{v} g_i(x, v)\left\{\int_0^{\infty}\sigma_2(|v\pm v'|)\,|v\pm v'|\,f^{-}(x, v')\,dv'\right. \\ & \left.+\int_0^{\infty}\sigma_2(|v\mp v'|)\,|v\mp v'|\,f^{+}(x, v')dv'\right\} \\ & \pm\frac{1}{2}\frac{n(x)}{v} g_i(x, v)\{\psi^{-}(x)\sigma_2(|v\pm v_0|)\,|v\pm v_0| \\ & +\psi^{+}(x)\sigma_2(|v\mp v_0|)\,|v\mp v_0|\}\,. \end{aligned} \tag{13}$$

The boundary condition at the centre of the plasma slab $x=0$ is derived from the symmetry of the model,

$$f^{+}(0, v) = f^{-}(0, v)\,. \tag{14}$$

Another boundary condition is assumed at $x=a$. This condition depends on the reflection of neutral particles by the wall (see Fig. 6). Since the reflection picture of the wall has not yet been clarified, we assumed that the energy distribution of the reflected neutral particles is not changed by the reflection, i.e.

$$f^{-}(a, v) = k\cdot f^{+}(a, v)\,. \tag{15}$$

Usually, the reflection coefficient k does not exceed unity.

The transport equation (13) can be solved numerically under the boundary conditions (14) and (15), if the plasma density $n(x)$, the ion temperature $T_i(x)$, and the electron temperature $T_e(x)$ are given. In this paper, the spatial distributions of the plasma parameters mentioned above are assumed as follows

(I)
$$\begin{aligned} n(x) &= n(1-\xi^2) \\ T_i(x) &= T_{i0}(1-\xi^4)^2+10 \\ T_e(x) &= 2T_i(x) \end{aligned}$$

and

(II) $n(x) = n(1-\xi^2)$

$T_i(x) = T_{i0}(1-\xi^2)+10$

$T_e(x) = 2T_i(x)$

where $\xi = x/a$.

4. Numerical solution of the transport equation

4.1 Derivation of the infinite difference equations

For the sake of simplicity, in addition to ξ, we introduce another dimensionless variable

$$u = v/v_t\,, \quad v_t = (2kT_{i0}/m_i)^{1/2}\,.$$

Moreover, we use the following substitutions

$$\langle\sigma v\rangle = \langle v\sigma\rangle_1+\langle v\sigma\rangle_2$$
$$q(\xi) = [T_i(\xi)/T_{i0}]^{1/2}$$
$$F^{\pm}(\xi, u) = \exp[-u^2]f^{\pm}(\xi, u)$$
$$h(\xi, u) = \exp[u^2]g_i(\xi, u) = \frac{1}{\sqrt{\pi}\, v_t q(\xi)} \exp[-u^2(1/q(\xi)-1)]\,.$$

Then the transport equation (13) can be written as

$$\begin{aligned}\frac{\partial F^{\pm}(\xi, u)}{\partial \xi} = {} & \mp\frac{an(\xi)}{uv_t}\langle\sigma v\rangle(\xi)F^{\pm}(\xi, u) \\ & \pm\frac{an(\xi)}{2u}h(\xi, u)\left\{\int_0^{\infty}\exp[-u'^2]\sigma_2(v_t|u\pm u'|)(v_t|u\pm u'|)F^{-}(\xi, u')du'\right. \\ & \left.+\int_0^{\infty}\exp[-u'^2]\sigma_2(v_t|u\mp u'|)(v_t|u\mp u'|)F^{+}(\xi, u')du'\right\} \\ & \pm\frac{an(\xi)}{2u}h(\xi, u)\{\psi^{-}(\xi)\sigma_2(v_t|u\pm u_0|)|u\pm u_0| \\ & +\psi^{+}(\xi)\sigma_2(v_t|\mp u_0|)|u\mp u_0|\}\,. \end{aligned} \tag{16}$$

We will derive the finite difference approximation of Eq. (16). Firstly, we apply the quadrature formula of the Gauss-Hermite type

$$\int_{-\infty}^{\infty}\exp[-u^2]f(u)du = \sum_{j=1}^{n} w_j f(u_j) \tag{17}$$

to the integrals on the right-hand side of Eq.(16). The quadrature points u_j and the weights w_j are given in reference 7).

Then we integrate Eq. (16) with respect to ξ in the range (ξ_{i+1}, ξ_i) and use the formula

$$\int_{\xi_i}^{\xi_{i+1}} f(\xi)d\xi = \frac{\Delta_i}{2}\{f(\xi_{i+1})+f(\xi_i)\}\ , \tag{18}$$

where $\Delta_i=\xi_{i+1}-\xi_i$. The mesh points ξ_i's are numbered from the centre toward the outer boundary: at $\xi=0$, $i=1$; $\xi=1$, $i=IMAX$.

If we write $F^{\pm}(i,j)$ instead of $F^{\pm}(\xi_i, u_j)$, then the finite difference equations for F^- and F^+ may be written as follows:

$$\begin{aligned} F^-(i,j) = \Big[\frac{2}{\Delta_i}F^-(i+1,j)+\sum_{j'=1}^{n}\{&A(i,j,j')F^-(i,j')+A(i+1,j,j')F^-(i+1,j') \\ &(j'=j \text{ excluded}) \\ &+B(i,j,j')F^+(i,j')+B(i+1,j,j')F^+(i+1,j')\} \\ &+C(i+1,j)\psi^-(i+1)+D(i+1,j)\psi^+(i+1)+C(i,j)\psi^-(i) \\ &+D(i,j)\psi^+(i)\Big]\Big[\frac{2}{\Delta_i}-A(i,j,j)\Big]^{-1} \end{aligned} \tag{19}$$

and

$$\begin{aligned} F^+(i+1,j) = \Big[\frac{2}{\Delta_i}F^+(i,j)+\sum_{j'=1}^{n}\{&B(i,j,j')F^-(i,j')+B(i+1,j,j')F^-(i+1,j') \\ &+A(i,j,j')F^+(i,j')+A(i+1,j,j')F^+(i+1,j')\} \\ &(j'=j \text{ excluded}) \\ &+C(i+1,j)\psi^+(i+1)+D(i+1,j)\psi^-(i+1)+C(i,j)\psi^+(i) \\ &+D(i,j)\psi^-(i,j)\Big]\Big[\frac{2}{\Delta_i}-A(i+1,j,j)\Big]^{-1}, \end{aligned} \tag{20}$$

where

$$A(i,j,j') = \frac{an(i)}{4u_j}h(i,j)\sigma_2(v_t|u_j-u_{j'}|)(v_t|u_j-u_{j'}|)W_{j'}-\delta_{jj'}\frac{an(i)}{2u_jv_t}\langle\sigma v\rangle,$$

$$B(i,j,j') = \frac{an(i)}{4u_j}h(i,j)\sigma_2(v_t|u_j+u_{j'}|)(v_t|u_j+u_{j'}|)W_{j'},$$

$$C(i,j) = \frac{an(i)}{4u_j}h(i,j)\sigma_2(v_t|u_j-u_0|)|u_j-u_0|,$$

$$D(i,j) = \frac{an(i)}{4u_j}h(i,j)\sigma_2(v_t|u_j+u_0|)|u_j+u_0|.$$

4.2 Iterative solution of the difference equations

The iterative solution is started from $i=IMAX$ with the initial guess $F^-(i,j)=0$ for all j. Using the backward difference Eq. (19), $F^-(i,j)$ is found for $i=IMAX-1$ through $i=1$. Then the boundary condition (14) gives the starting value for

the forward difference Eq. (20), i.e. $F^+(1,j)=F^-(1,j)$. Hence $F^+(i,j)$ can be calculated from $x=0$ $(i=1)$ toward $x=a$ $(i=IMAX)$. The iteration is repeated with starting value $F^-(IMAX,j)=k\cdot F^+(IMAX,j)$ until it converges.

For judging the convergence, we define a ratio c by

$$c=\frac{v_t^2\sum_j W_j u_j F^+(IMAX,j)}{v_0\psi^-(a,v_0)+v_t^2\sum_j W_j u_j F^-(IMAX,j)}\,. \tag{21}$$

This ratio represents the probability that the neutrals immerging into the plasma ultimately escape from the surface in the form of neutral particles. The convergence criterion is

$$\left|\frac{c_n-c_{n-1}}{c_n}\right|<\varepsilon\,, \tag{22}$$

where c_n is the value of c after n-th iteration. The convergence of this problem was rather rapid. When $\varepsilon=10^{-3}$, the number of the iteration was only 3 or 4.

4.3 Energy spectrum of neutral paticle flux

The energy spectrum of neutral particles emerging from the plasma coulmn is measured by using a multi-channel energy analyzer in practice. The counting rate of the analyzer is proportional to the intensity of the outward flux at the surface $(x=a)$ of the plasma. The energy spectrum of the neutral particle flux $\phi(x,E)$ is obtained from the distribution function $f(x,v)$ by the relation

$$\phi(x,E)=vf(x,v)\frac{dv}{dE}=\frac{1}{m_i}f(x,v)\,. \tag{23}$$

The energy spectrum of the neutral particles emerging from the plasma is given by $\phi^+(x=a,E)$. The spectrum $\phi^+(a,E)$ determined numerically from the transport equation (13) is apparently described by the following equation

$$\log\phi^+(a,E)=\text{transient term}-\frac{E}{T^*}+b\,,$$

where b is a constant. The transient term decreases rapidly, and for energies above $5E_0$ $(E_0=T_{i0})$, the spectrum can well be represented by the asymptotic form

$$\log\phi^+(a,E)=-\frac{E}{T^*}+b\,,$$

which is a Maxwellian distribution with the temperature T^*. We call T^* an asymptotic temperature. The asymptotic temperature has been calculated at

the energies E_1 and E_2, which are about 6.6 and 9 times as high as the maximum ion temperature, respectively, i.e.

$$T^* = \frac{E_2 - E_1}{\log \phi^+(a, E_1) - \log \phi^+(a, E_2)} . \tag{24}$$

As mentioned earlier in Section 1, the asymptotic temperature T^* is considered to have a close correlation with the ion temperature $T_i(0)$, the density $n(0)$, and the half-thickness a of the plasma. It should be noticed that the transport equation (16) contains the product $a \cdot n$, but not the individual factor a or n. Numerical results will be shown in the next section. The emerging neutral flux is normalized with respect to the immerging slow neutral flux by the relation

$$v_0 \psi^-(a, v_0) = 1 .$$

5. Numerical nesults

5.1 Influence of the reflection coefficient of the wall on the neutral density profile and the spectra of the emerging neutral flux

The influence of the wall condition on the neutral density profile and the spectra of the emerging neutral flux has been studied by changing the reflection coefficient of the wall. Figure 7 shows the neutral density profiles in a plasma

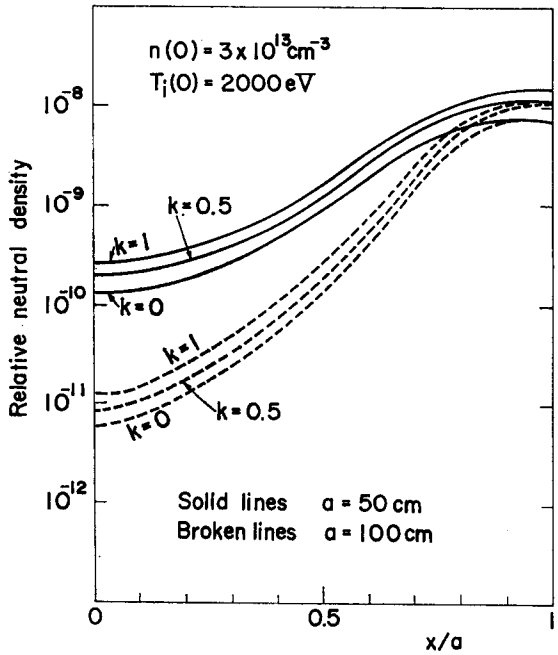

Fig. 7. Spatial distribution of neutral density with the reflection coefficient of the wall as a parameter.

whose density and maximum ion temperature are $n(0)=3\times10^{13}\,\mathrm{cm}^{-3}$ and $T_i(0)=$ 2000 eV, respectively. The solid lines in Fig. 7 are for the plasma of $a=50$ cm ($a\cdot n(0)=1.5\times10^{15}\,\mathrm{cm}^{-2}$), while the broken lines are for $a=100$ cm ($a\cdot n(0)=3\times10^{15}\,\mathrm{cm}^{-2}$). In both cases, we assumed three distinctly different values of the reflection coefficient of the wall: 0, 0.5 and 1. We can see from Fig. 7 that the neutral density shows a slight increase with the increased reflection coefficient. However, no important changes have been noticed in their profiles.

Figure 8 shows the effect of the reflection coefficient of the wall to the emerging neutral spectra. In Fig. 8, curves 1 and 2 represent the spectra of neutrals emerging from a plasma whose parameters are $a=25$ cm, $n(0)=10^{13}\,\mathrm{cm}^{-3}$ ($a\cdot n(0)=0.25\times10^{15}\,\mathrm{cm}^{-2}$) and $T_i(0)=300$ eV. For the reflection coefficient of the wall, the extreme values zero and unity are assumed. The asymptotic temperature calculated

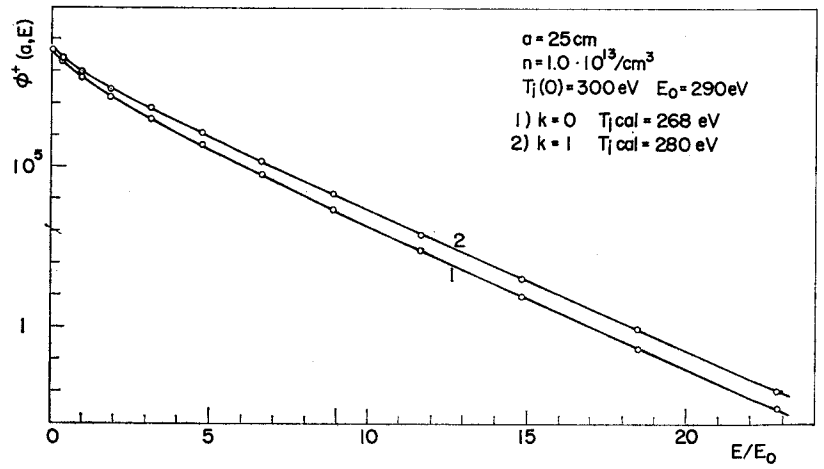

Fig. 8. Spectra of emerging neutral flux from a plasma with the reflection coefficient of the wall as a parameter. ($T_{i\,\mathrm{cal}}=T^*$)

from curve 1 is about 268 eV which is 89 % of the maximum ion temperature of plasma $T_i(0)$, while that from curve 2 is about 280 eV which is 93 % of $T_i(0)$. Hence, we can say that for the parameter of the plasma shown in Fig. 8, the effect of the wall reflection coefficient to the emerging neutral spectra is not significant. It influences the estimation of $T_i(0)$ from the emerging neutral spectra within a changing range of about 5 %. However, as we can see from Fig. 8, the intensity of the outgoing neutral flux spectrum 2 ($k=1$) is 2–3 times greater than that of spectrum 1 ($k=0$).

Since the reflection coefficient of the wall does not contribute any significant effect to the emerging neutral spectra nor to the asymptotic temperature calculated

from the slope of the spectra, we mainly show the results obtained under the wall condition of zero-reflection.

5.2 Influence of the plasma density and the spatial distribution of ion temperature on the spectra of emerging neutral flux

Figure 9 shows the emerging neutral flux spectra from a plasma whose half-thickness a is 50 cm and whose maximum ion temperature $T_i(0)$ is 5000 eV, with the plasma density as a parameter. The wall reflection coefficient is assumed to be zero. We can see from Fig. 9 that the intensity of the emerging neutral flux decreases with an increasing plasma density. Moreover, the asymptotic temperature also decreases with an increasing plasma density.

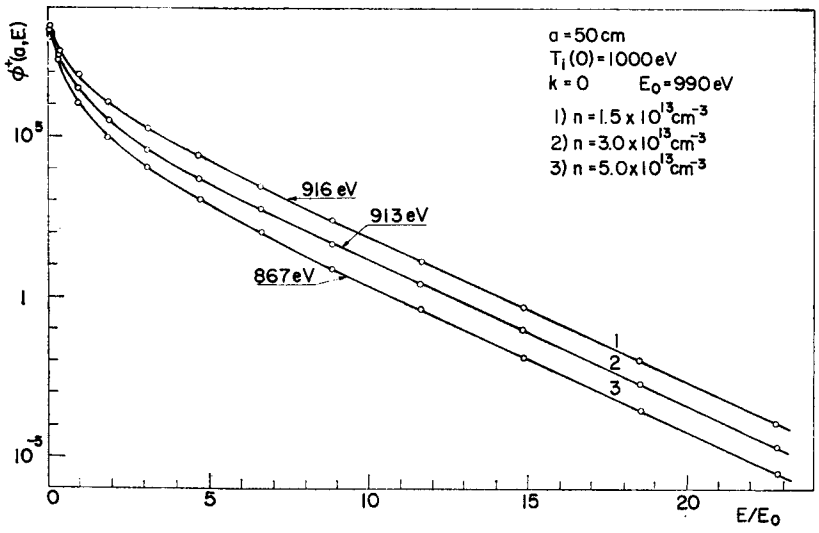

Fig. 9. Spectra of emerging neutral flux from a plasma with the plasma density as a parameter.

Figure 10 shows the emerging neutral flux spectra from a plasma whose parameters are $a=100$ cm, $n(0)=3\times10^{13}$ cm^{-3} and $T_i(0)=5000$ eV, for two different spatial distributions of ion temperatures. Spectra 1 and 2 in Fig. 10 are the emerging neutral flux spectra from the plasmas whose parameter distributions are, respectively, (I) and (II) as mentioned in Section 3. Namely, for spectrum 1 in Fig. 10, the spatial distribution of the plasma density is parabolic, and that of the ion temperature is proportional to $(1-\xi^4)^2$, while for spectrum 2, all these spatial distributions are parabolic. It is obvious that the difference in the spatial distribution of ion temperatures just slightly influences the emerging neutral spectra.

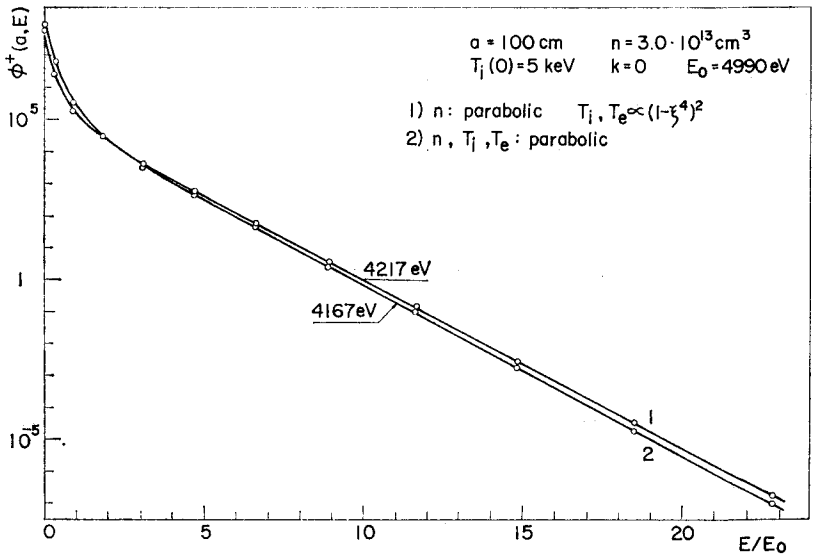

Fig. 10. Spectra of emerging neutral fluxx from a plasma for the parabolic and non-parabolic profiles of the ion temperature.

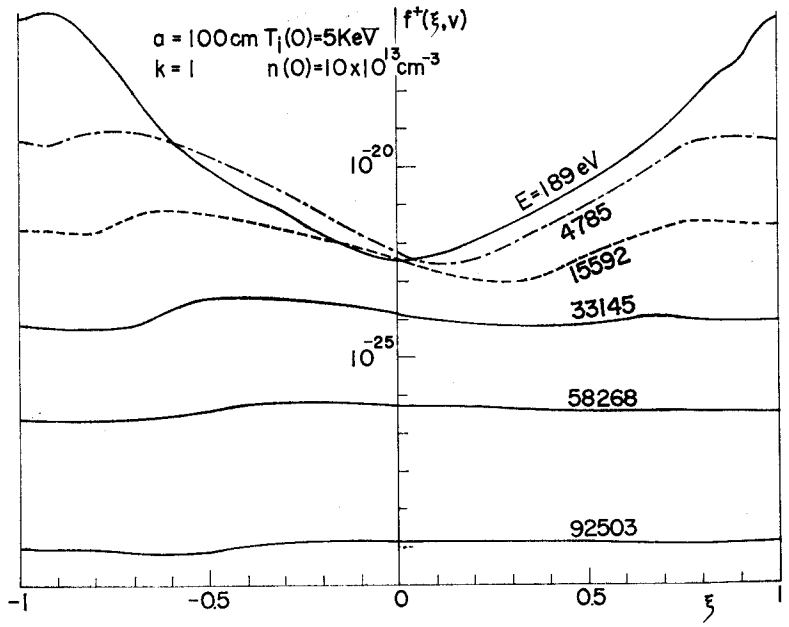

Fig. 11. Density profiles of the right-ward neutral particles with several representative energies.

Figure 11 shows the density profiles of the right-ward neutral particles with some representative energies in a plasma whose parameters are $a=100\,\mathrm{cm}$, $n(0)=10\times10^{13}\,\mathrm{cm}^{-3}$ ($a\cdot n(0)=10^{16}\mathrm{cm}^{-2}$), $T_i(0)=5000\,\mathrm{eV}$, and the reflection coefficient of the wall $k=1$. We can notice from Fig. 11 that the spatial distribution of the low energy neutral particles decays rapidly from the surface toward the centre of the plasma. However, the higher energy neutral particles distribute more uniformly, because of their longer decay lengths.

5.3 Asymptotic temperature calculated from the spectrum of emerging neutral flux of a plasma

As mentioned previously, the asymptotic temperature T^* is calculated by Eq. (24). Figures 12 and 13 show some correlation between the asymptotic temperature T^* and the maximum ion temperature $T_i(0)$.

Figure 12 shows the ratio η as a function of $T_i(0)$ with the wall reflection coefficient k as a parameter, and the product $a\cdot n(0)$ is assumed to be 0.375×10^{15} cm^{-2}. Within the ion temperature range shown in Fig. 12, the ratio η is almost constant.

Figure 13 illustrates the asymptotic temperature as a function of $T_i(0)$ with the product $a\cdot n(0)$ as a parameter. It is obvious that the asymptotic temperature is generally less than the maximum ion temperature of the plasma, and decreases with the increasing product $a\cdot n(0)$.

Figure 14 shows the escape probability c of Eq. (21) as a function of the maximum ion temperature $T_i(0)$, with the product $a\cdot n(0)$ as a parameter. The

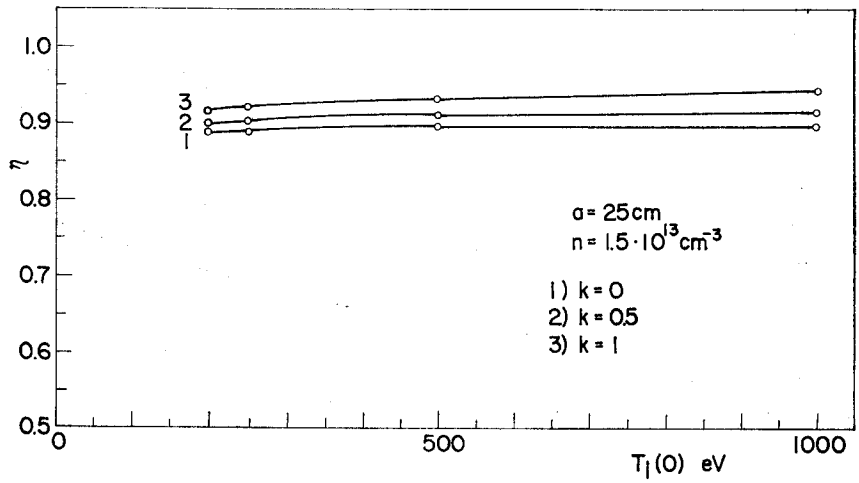

Fig. 12. Asymptotic temperature as a function of the maximum ion temperature of the plasma with the reflection coefficient of the wall as a parameter.

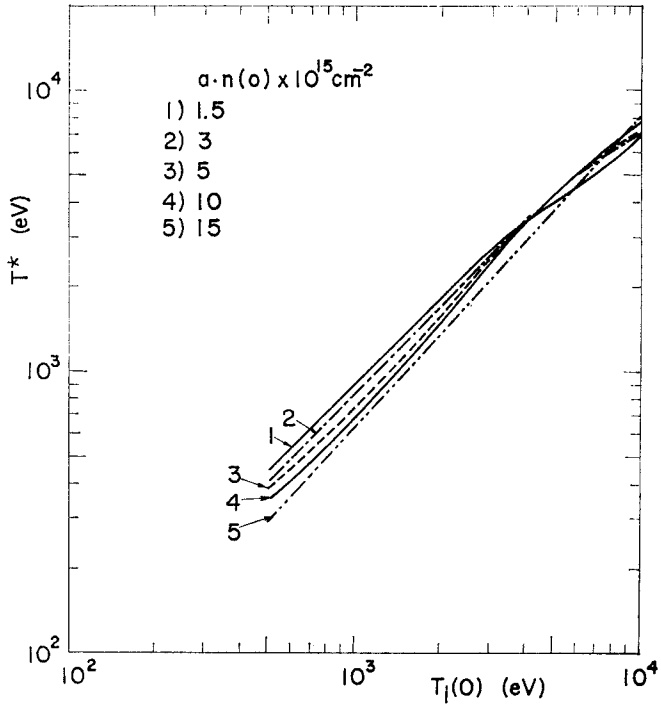

Fig. 13. Asymptotic temperature as a function of maximum ion temperature of the plasma with the product $a \cdot n(0)$ as a parameter.

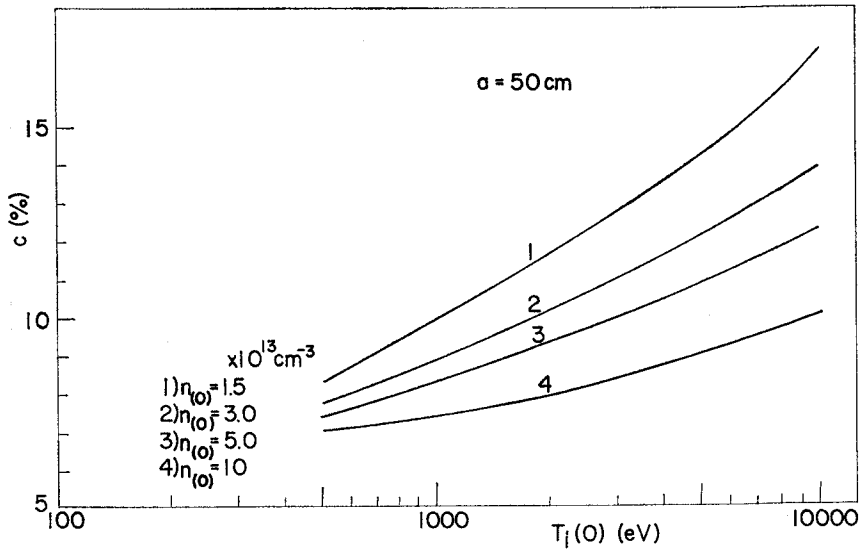

Fig. 14. Escape probability of the immerging neutral particles as a function of the maximum ion temperature of the plasma with the product $a \cdot n(0)$ as a parameter.

probability c incresaes with a increasing ion temperature of the plasma, but decreases with the increasing product $a \cdot n(0)$. Within the ranges of the plasma parameters assumed, c does not exceed 20 %. In view of the particle conservation in a plasma of stationary state, the remainder of the incoming neutrals must be ionized by the plasma particles and be diffused from the plasma in the form of ions.

6. Discussion

The cross-section for ionization of atomic hydrogen by protons is given by Eqs.(10) and (11) and shown in Fig.3. The threshold of this interaction seems to be very high. In fact, there are no experimental data for energies below 7 keV. For instance, if Eq. (10) is still sound at 1 keV, the cross-section is of the order of $10^{-19}\,\mathrm{cm}^2$. Since this cross-section is much smaller than that of the charge-exchange, we have not considered it in the present calculation.

However, above 10 keV, the cross-section for the ionization of atomic hydrogen by protons becomes comparable with the charge-exchange cross-section or even larger. Therefore, it is worth estimating the effect caused by this interaction on the emerging neutral flux. Figures 15(a) and (b) illustrate the effect of the ionization of atomic hydrogen by protons on the spectra of emerging neutral flux. Figure 15(a) shows the spectra of emerging neutral flux from a plasma whose parameters are $a \cdot n(0) = 3 \times 10^{15}\,\mathrm{cm}^{-2}$ and $T_i(0) = 2$ keV, the reflection coefficient of the wall being zero. Curve 1 in Fig. 15(a) is obtained by taking only the reactions of Eqs.(5) and (6) into account, while curve 2 is the result including the reaction of neutrals being ionized by protons. Spectrum 1 is a little larger than spectrum 2 in the higher energy region, but they coincide below 6 keV. The difference between the respective asymptotic temperatures is within 3 %. Therefore, it is tolerable for us to ignore the ionization of neutrals by protons in determining the asymptotic temperature.

7. Conclusions

1) Figure 13 shows that the asymptotic temperature T^* of the fast neutral particles emerging from a high temperature plasma slab depends primarily on the central ion temperature $T_i(0)$, and secondly on the product of the half-thickness a and the central plasma densfty $n(0)$. The ratio $\eta = T^*/T_i(0)$ is not significantly influenced by the profile of the ion temperature distribution.

2) For $T_i(0)$ less than about 4 keV, the ratio η decreases with an increasing $a \cdot n(0)$, while for $T_i(0)$ above about 4 keV, it increases with an increasing $a \cdot n(0)$.

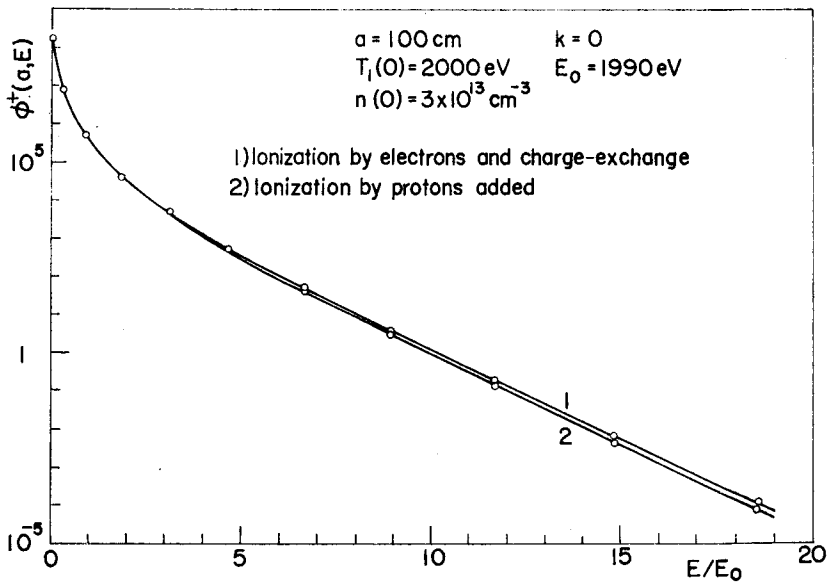

(a)

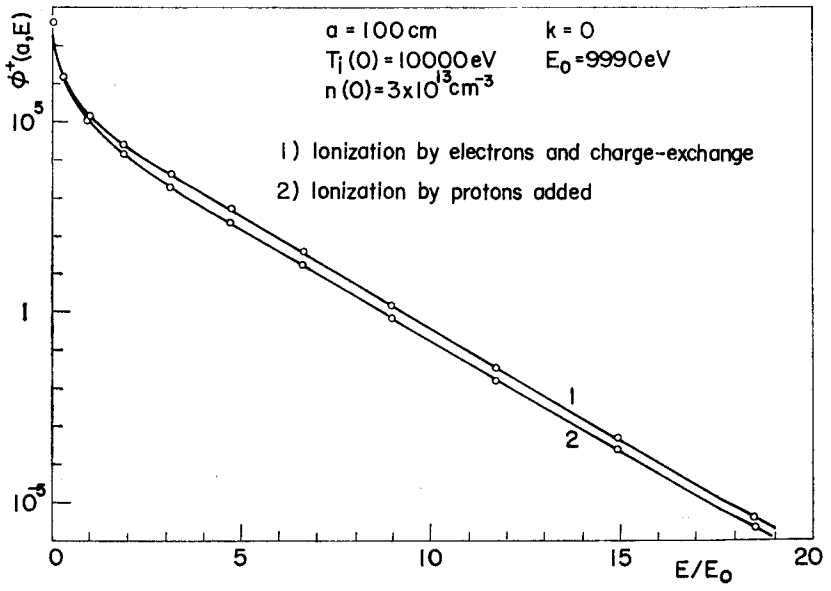

(b)

Figs. 15(a) and (b). Effect of the ionization of atomic hydrogen by protons on the spectrum of emerging neutral flux.

3) For practically realizable values of plasma parameters, the ratio η is within the the range of 0.7 to 0.95.

4) By experimentally determining the asymptotic temperature, and using its correlation with the plasma parameters, we can estimate the maximum ion temperature of a plasma.

5) The reflection coefficient of the wall does not play an important role for the spectrum of the emerging neutral flux. However, it can effectively influence the intensity of the emerging neutral flux.

Acknowledgement

Yip (one of the authors), would like to thank Mr. A. Kitamura and Dr. T. Takitsuka for their helpful discussions. He is also grateful to Drs. J. Horie and N. Ohtani for their help in improving the FORTRAN program.

The computation was performed at the Data Processing Center of Kyoto University.

References

1) V.V. Afrosimov, and M.P. Petrov, Soviet Phys.-Tech Phys., **12**, 1467 (May, 1968).
2) L.A. Artsimovich, Nucl. Fusion **12**, 215 (1972).
3) Y.N. Dnestrovskii, D.P. Kostomarov, and N.L. Pavlova, MATT-TRANS 107, (December, 1971).
4) S. Rehker, and H. Wobing, IPP2/208 (January, 1973).
5) A.C. Riviere, Nucl. Fusion **11**, 363 (1971).
6) J.B. Hasted, Physics of Atomic Collisions, 2nd ed., London, Butterworths, 612 (1972).
7) A.H. Stround and Don Secrest, Gaussian Quadrature Formulas, Prentice-Hall, Inc., Englewood Cliffs, N.J. 218 (1966).